Collective excitations of semi-infinite superlattice structures: Surface plasmons, bulk plasmons, and the electron-energy-loss spectrum

R. E. Camley
Department of Physics and Energy Science, University of Colorado, Colorado Springs, Colorado 80907

D. L. Mills
Department of Physics, University of California, Irvine, California 92717
(Received 8 August 1983)

We consider a semi-infinite superlattice structure, with constituent A characterized by dielectric constant $\epsilon_A(\omega)$ and constituent B by $\epsilon_B(\omega)$, and examine collective excitations of the system in the absence of retardation effects. Also, we explore the energy-loss spectrum of electrons backscattered from such a structure. Detailed application is to the case where one constituent, a semiconductor or metal, contains free carriers, while the second is described by a frequency-independent dielectric function. Surface excitations (surface plasmons) on adjacent interfaces couple through macroscopic electric fields to form a propagating band of collective excitations of the whole structure capable of transporting energy normal to the interfaces. We then find surface excitations of the entire structure. These are linear superpositions of modes localized at successive interfaces, combined with an envelope function which decays exponentially as one moves down the stack. By explicit calculations of the energy-loss spectrum, we show how electron-energy-loss spectroscopy may be used to study these and other collective modes of the array.

I. INTRODUCTION

Recently there has been considerable interest in the properties of superlattices, which are structures composed of alternating layers of different materials. Typically the thickness of an individual layer lies in the range 100—5000 Å. If one constituent, material A, always has thickness d_1, and the second, material B, always has thickness d_2, one has built a periodic structure known as a superlattice.

Superlattices composed of semiconducting materials have been studied extensively. Here electrons may be trapped on the near vicinity of the interfaces by band-bending effects, to form a thin, two-dimensional gas. More recently, metallic superlattices have been fabricated,[1] and their elastic properties have been studied. One may also fabricate structures which consist of alternating layers of magnetic and nonmagnetic metals.

Most studies of the semiconducting superlattices suppose the material consists of parallel sheets of free carriers, each independent of the other. The superlattice structure than allows access to the two-dimensional electron gas, under conditions where the average volume density is rather high, which is convenient from the experimental point of view.

One may inquire if there are collective excitations of the whole superlattice structure, with properties distinct from those characteristic of either constituent. The answer is clearly in the affirmative. Some years ago, Fetter[2] considered the elementary excitations of an infinitely extended stack of two-dimensional plasmas. Excitation of a plasmon within one constituent produces electric fields which extend outside its boundaries, and these fields couple the elementary excitations of the various layers. Through use of Bloch's theorem, one then sees that a consequence of this coupling is a set of collective plasma excitations of the whole superlattice structure, characterized by a wave vector normal to the interfaces; these modes may thus transmit energy normal to the layers of the superlattice structure.

Recently, the collective spin-wave excitations of semi-infinite magnetic superlattices have been studied theoretically,[3,4] and a striking prediction emerges from these analyses. First of all, on each interface between a ferromagnet and its nonmagnetic partner, one has surface spin waves, and surface spin waves on adjacent interfaces couple through dipolar fields generated by the spin motion, very much as in Fetter's study of plasmons. When the superlattice is terminated, of course each normal mode of the structure (this is a linear combination of surface spin waves, combined via the Bloch theorem to form a propagating mode of the whole structure) may propagate to the surface, to reflect off of it. In addition, one finds a surface mode of the semi-infinite superlattice.[3,4] This is a linear combination of surface spin waves, combined with an envelope function which decays exponentially as one moves into the stack. This mode has the remarkable property that its frequency is exactly that of the surface mode appropriate to a semi-infinite ferromagnet, though its wave function is clearly very different. If d_1 is the thickness of the magnetic constituent, and d_2 that of the nonmagnetic layers, the surface mode exists only when $d_1 > d_2$. As $d_1 \to d_2$ from above, the surface mode merges with the "bulk" excitations of the system, and is absent when $d_1 < d_2$. Experimental studies of spin waves in these materials by Brillouin scattering confirm these predictions.[5]

The present paper presents analysis of a semi-infinite superlattice, which consists of alternating layers of material, where one or both constituent contains free carriers, or possibly electric-dipole-active collective excitations such as optical phonons or excitons. We inquire if a semi-infinite structure of such materials may support a surface excitation similar to the spin wave described in the preceding paragraph, and find the answer to be yes, under the conditions outlined below. We argue that one should be able to observe such modes by means of electron-energy-loss spectroscopy, and we present an analysis of the electron-energy-loss spectrum in a backscattering geometry to illustrate this point.

The paper is organized as follows. Section II presents the theory for both the "surface" and "bulk" collective modes of the structure just described, and we derive the dispersion relations of the various modes. Numerical results are then presented for particular structures. In Sec. III we present the theory of the electron-energy-loss cross section, and Sec. IV is devoted to a summary of our principal conclusions, including the numerical studies of the electron-energy-loss cross section.

II. DISPERSION RELATIONS AND GENERAL PROPERTIES OF ELECTRIC-DIPOLE-ACTIVE COLLECTIVE EXCITATIONS OF SUPERLATTICE STRUCTURES

It is useful to break the discussion of the present section into several parts. We consider first a review of the collective modes of an isolated dielectric slab, then turn to a superlattice structure of infinite extent, and next the terminated superlattice. Then we proceed to some numerical examples.

A. Isolated slab

For what follows, it will be useful to consider those collective excitations of an isolated dielectric slab (possibly a metal) which in the long-wavelength limit generate a macroscopic electric field. Then if we confine our attention to only this limit of long wavelengths, the mode structure is described fully by macroscopic theory. Suppose the slab has thickness d, vacuum above and below, and has a frequency-dependent dielectric constant $\epsilon(\omega)$, assumed real in this section. The macroscopic electric field associated with the elementary excitations of interest may be derived from an electrostatic potential $\phi(\vec{x},t)$; throughout this paper, we ignore retardation,[6] so $\phi(\vec{x},t)$ obeys Laplace's equations everywhere outside the slab,

$$\nabla^2\phi(\vec{x},t)=0 . \tag{2.1a}$$

Then inside the slab we have

$$\epsilon(\omega)\nabla^2\phi(\vec{x},t)=0 . \tag{2.1b}$$

In general, an excitation in the slab will set up a fluctuating electric field in the vacuum above and below it. We denote the electrostatic potentials in these two regions by $\phi^>$ and $\phi^<$, respectively, and that within the slab by ϕ_i.

Translational invariance parallel to the two surfaces ensures that all elementary excitations are characterized by a two-dimensional wave vector $\vec{k}$ parallel to the surfaces. Without loss of generality, we may chose $\vec{k}$ directed along the $\vec{x}$ axis. Then the electrostatic potential everywhere has the form

$$\phi(\vec{x},t)=\Phi(z)e^{i(kx-\omega t)} . \tag{2.2}$$

We then have the following two distinct sets of elementary excitations which generate a macroscopic field.

(i) *Surface excitations.* An isolated dielectric-vacuum interface supports a surface excitation with a frequency independent of wave vector $\vec{k}$, at any frequency ω_s for which $\epsilon(\omega_s)=-1$. If the interface coincides with the plane $z=0$, the electrostatic potential falls to zero exponentially, as one moves away from the interface in either direction. One has $\Phi(z)\sim\exp(-k\,|z\,|)$ for such modes.

The finite slab, considered very thick for the moment, supports two such modes, one on each surface. With a thickness finite, the two modes couple to produce an odd- or even-parity pair, split by interaction between the two surfaces. We thus have dispersion relations $\omega_-(k)$ and $\omega_+(k)$, respectively.

The ω_- mode is described by the implicit dispersion relation

$$\epsilon(\omega_-)=-\coth(\tfrac{1}{2}kd) . \tag{2.3a}$$

If $\epsilon(\omega)=\epsilon_\infty+\Omega_p^2/(\omega_0^2-\omega^2)$, then as $kd\to\infty$, $\omega_-(k)$ approaches the single-interface surface-mode frequency $\omega_s=\omega_0^2+\Omega_p^2/(1+\epsilon_\infty)$, while as $kd\to0$, $\omega_-(k)\to\omega_0$, where $\epsilon(\omega)$ is infinite. If we have a metal, then $\omega_0=0$, and so $\omega_-(k)\to0$ as $kd\to0$, with $\omega_-(k)=\Omega_p(\frac{1}{2}kd)^{1/2}$ when $kd\ll1$. This mode is an odd-parity mode in the sense that the electrostatic potential is odd under reflection through the midpoint of the film.

The ω_+ mode has the implicit dispersion relation

$$\epsilon(\omega_+)=-\tanh(\tfrac{1}{2}kd) . \tag{2.3b}$$

Then as $kd\to\infty$, $\omega_+(k)$ also approaches ω_s, while as $kd\to0$, $\omega_+(k)$ approaches the frequency for which $\epsilon(\omega)$ vanishes. This is the LO-phonon frequency in a simple ionic insulator, or the bulk-plasma frequency for a metal. The electrostatic potential has even parity under reflection through the midpoint of the film.

The results above are well known, and may be derived in a few lines by noting that $\phi(\vec{x}t)$ satisfies Laplace's equation everywhere, including inside the film [because $\epsilon(\omega)\neq0$]. Then by requiring that ϕ be continuous at each interface along with normal components of $\vec{D}=\epsilon(\omega)\vec{E}$, constraints which lead to the dispersion relations follow.

(ii) *Bulk excitations.* An infinitely extended dielectric medium supports bulk excitations of longitudinal character (plasmons, LO phonons, and longitudinal excitions) at those particular frequencies where $\epsilon(\omega)\equiv0$. Here we are no longer constrained to have $\nabla^2\phi=0$ within the medium, since $\epsilon(\omega)$ vanishes in Eq. (2.1b). For the slab, elementary arguments given elsewhere[7] serve to delineate the properties of the bulk excitations of a finite slab. One has a sequence of standing-wave resonances of the slab, each with frequency such that $\epsilon(\omega)\equiv0$, i.e., the frequency of each

slab resonance is identical to that of the relevant bulk excitation. The boundary conditions require $\phi^{>}(\vec{x}t)$ and $\phi^{<}(\vec{x},t)$ vanish identically, so the modes generate no macroscopic electric field outside the slab itself. If the slab surfaces are located in the planes $z=0$ and $z=d$, then $\Phi(z)\sim\sin(n\pi z/d)$, so there is a macroscopic field of standing-wave character within the slab. These conclusions will be altered by the presence of spatial dispersion effects not examined here; these will be small in the long-wavelengths limit and in a number of geometries of practical interest.

B. Superlattice of infinite extent

We consider here the structure shown in Fig. 1. Material A has a frequency-independent dielectric constant $\epsilon_A(\omega)$, and thickness d_1, while material B has a dielectric constant $\epsilon_B(\omega)$ and thickness d_2. For the purposes of the present discussion, $\epsilon_A(\omega)$ and $\epsilon_B(\omega)$ will be supposed real; this restriction is relaxed later in the paper. The "unit cells" of the structure are designated by the index n, as illustrated in the figure.

As we saw in the preceding subsection, an isolated slab of material A or B has standing-wave resonances (bulk LO phonons, bulk plasmons, etc.) which generates a macroscopic electric field at any frequency for which $\epsilon_A(\omega)$ or $\epsilon_B(\omega)$ vanishes. The electric field associated with such excitations is totally confined within the slab, so when a superlattice such as that in Fig. 1 is constructed, each constituent still possesses bulk resonances identical to those in the isolated film. These are unaffected by the fact that the film in question is now incorporated into a superlattice structure.

Here we study the collective excitations of the whole structure which have frequency ω such that neither $\epsilon_A(\omega)$ nor $\epsilon_B(\omega)$ vanish. The electrostatic potential $\phi(\vec{x},t)$ then satisfies Laplace's equation everywhere,

$$\nabla^2\phi(\vec{x},t)=0\ , \tag{2.4}$$

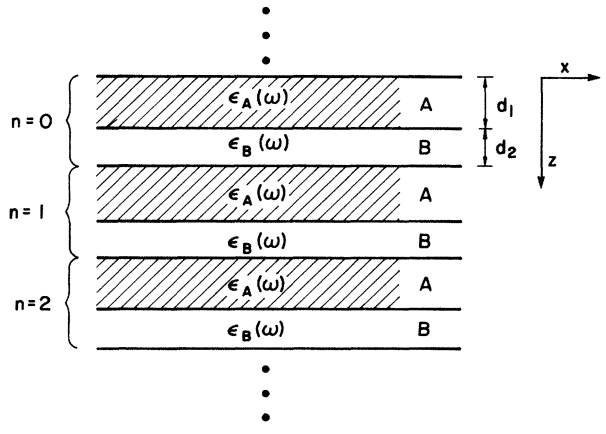

FIG. 1. Infinitely extended superlattice. The structure is made of alternating layers of material A and B, each characterized by the relevant dielectric constant. The unit cells of the structure are indexed by n, as illustrated.

and must obey appropriate boundary conditions at each interface.

Since we have translational invariance in the two directions normal to the z axis, each normal mode is characterized by a two-dimensional wave vector $\vec{k}$ parallel to the xy plane, as in the case of the isolated slab. We assume each material is isotropic, so that without loss generality, $\vec{k}$ may be taken parallel to the x axis. Thus, $\phi(x,y,z,t)$ will have the form

$$\phi(x,y,z,t)=\Phi(z)e^{i(kx-\omega t)}\ , \tag{2.5}$$

and Eq. (2.4) leads to

$$\left[\frac{d^2}{dz^2}-k^2\right]\Phi(z)=0\ . \tag{2.6}$$

Quite clearly, the general solution of this simple equation is

$$\Phi(z)=A_+e^{+kz}+A_-e^{-kz}\ . \tag{2.7}$$

Since the structure in Fig. 1 is periodic in the z direction, our task is to synthesize the basic solutions in Eq. (2.7) so that proper boundary conditions are satisfied at each interface, and so that the solution forms a Bloch wave, with respect to translations normal to the interface. Thus, if $L=d_1+d_2$ is the length of a unit cell, we require that $\Phi(z)$ be written in the form

$$\Phi(z)=e^{iqz}U_q(z)\ , \tag{2.8}$$

where for any integer n,

$$U_q(z+nL)=U_q(z)\ . \tag{2.9}$$

First consider the form of the electrostatic potential within the nth slab of material A, which extends from $z=nL$ to $z=nL+d_1$. One readily verifies that the most general solution of Eq. (2.6) which also satisfies Eq. (2.9) may be written

$$U_q(z)=e^{-iq(z-nL)}(A_+e^{k(z-nL)}+A_-e^{-k(z-nL)})\ , \quad nL\le z\le nL+d_1 \tag{2.10}$$

so that we have

$$\Phi(z)=e^{iqnL}(A_+e^{k(z-nL)}+A_-e^{-k(z-nL)})\ . \tag{2.11}$$

In this discussion, q is a wave vector that will ultimately enter the dispersion relation of the collective excitations of the superlattice.

Similarly, one may write the most general form of the scalar potential within the nth layer of medium B, which extends from $z=nL+d_1$ to $z=(n+1)L$. We have

$$\Phi(z)=e^{iqnL}(B_+e^{k(z-nL-d_1)}+B_-e^{-k(z-nL-d_1)})\ . \tag{2.12}$$

There are four arbitrary constants, A_+, A_-, B_+, and B_-, which appear in the scalar potential. To constrain these and obtain an explicit dispersion relation for the collective excitations we require that boundary conditions at the various interfaces be obeyed. These are that the electrostatic potential be continuous across each interface, along with normal components of $\vec{D}$. Through the use of the above forms, we apply these at $z=nL$ and $z=nL+d_1$,

and the Bloch property of the basic solution insures they are satisfied everywhere else.

Continuity of $\Phi(z)$ at $z=nL+d_1$, along with normal $\vec{D}$, gives the two constraint equations

$$A_+e^{+kd_1}+A_-e^{-kd_1}=B_++B_- \tag{2.13}$$

and

$$\epsilon_A(\omega)(A_+e^{+kd_1}-A_-e^{-kd_1})=\epsilon_B(\omega)(B_+-B_-)\,, \tag{2.14}$$

while the same conditions applied at $z=nL$ give

$$A_++A_-=e^{-iqL}(B_+e^{kd_2}+B_-e^{-kd_2}) \tag{2.15}$$

and

$$\epsilon_A(\omega)(A_+-A_-)=\epsilon_B(\omega)e^{-iqL}(B_+e^{kd_2}-B_-e^{-kd_2}). \tag{2.16}$$

By setting the appropriate 4×4 determinant formed from Eqs. (2.13)–(2.16) to zero, we obtain an implicit dispersion relation for the collective modes of the superlattice. This reads

$$\left[1+\left[\frac{\epsilon_A(\omega)}{\epsilon_B(\omega)}\right]^2\right]\sinh(kd_2)\sinh(kd_1) +2\frac{\epsilon_A(\omega)}{\epsilon_B(\omega)}[\cosh(kd_2)\cosh(kd_1)-\cos(qL)]=0\,. \tag{2.17}$$

In general, this implicit dispersion relation must be solved numerically. For fixed k, this yields the frequency ω as a function of q, the wave vector of the collective excitation in the direction normal to the stack. If we define

$$c(k,q)=\frac{\cosh(kd_2)\cosh(kd_1)-\cos(qL)}{\sinh(kd_2)\sinh(kd_1)}\,, \tag{2.18}$$

a positive definite quantity for any choice of k or q, then Eq. (2.17) admits solutions whenever

$$\frac{\epsilon_A(\omega)}{\epsilon_B(\omega)}=-c(k,q)\pm[c^2(k,q)-1]^{1/2}\,. \tag{2.19}$$

For the frequencies which emerge from Eq. (2.19) to be real, we must append the condition

$$c(k,q)\geq1\,. \tag{2.20}$$

It is then convenient to parametrize $c(k,q)$ by writing

$$c(k,q)=\cosh\psi(k,q)\,, \tag{2.21}$$

where, when Eq. (2.20) is satisfied, $\psi(k,q)$ is real. The implicit dispersion relation in Eq. (2.19) then reads

$$\frac{\epsilon_A(\omega)}{\epsilon_B(\omega)}=-\exp[\pm\psi(k,q)]\,, \tag{2.22}$$

so that our collective excitations occur only in frequency regimes where the ratio $\epsilon_A(\omega)/\epsilon_B(\omega)$ is *negative*.

The frequency regime where $\epsilon_A(\omega)/\epsilon_B(\omega)$ is negative is, in fact, the spectral region where surface polaritons may propagate on the interface between medium A and B. The collective excitations discussed here may be viewed as a linear superposition of surface polaritons, one localized at each interface in Fig. 1. When d_1 and d_2 are finite, they couple because their fields overlap, resulting in normal modes of the whole structure. Their nature is controlled by Bloch's theorem, which dictates the form assumed by the resulting electrostatic potential.

Suppose $kd_1\gg1$ with kd_2 finite, i.e., let $d_1\to\infty$ with d_2 fixed. Then one readily sees that Eq. (2.19) degenerates to

$$\frac{\epsilon_B(\omega)}{\epsilon_A(\omega)}=-\begin{cases}\coth(\frac{1}{2}kd_2)\\ \tanh(\frac{1}{2}kd_2)\,,\end{cases} \tag{2.23}$$

the generalization of Eqs. (2.3) to the case where a finite slab of material B of thickness d_2 is embedded in medium A. Of course, Eq. (2.19) is symmetric under interchange of d_1 and d_2, so that if $d_2\to\infty$ with d_1 finite, we obtain the dispersion relation of the surface modes of a slab of medium A with thickness d_1 embedded in medium B.

Explicit expressions for the dispersion relations may be obtained for a variety of special cases. For example, let

$$\epsilon_A(\omega)=\epsilon_A^{(\infty)}+\frac{\Omega_p^2}{\omega_0^2-\omega^2}\,, \tag{2.24}$$

so that material A is possibly a polar semiconductor or a nearly-free-electron metal ($\omega_0\to0$). Then let $\epsilon_B(\omega)=\epsilon_B^{(\infty)}$, corresponding to a nonpolar semiconductor or an insulator. Then we have

$$\omega_\mp^2(k,q)=\omega_0^2+\frac{\Omega_p^2}{\epsilon_A^{(\infty)}+\epsilon_B^{(\infty)}\exp[\pm\psi(k,q)]}\,. \tag{2.25}$$

The model considered above has three characteristic frequencies. The first is ω_0, which is the TO-phonon frequency if we view material A as a polar material. Then we have the LO-phonon frequency of material A, given by $\omega_0^2+\Omega_p^2/\epsilon_A^{(\infty)}$, and finally there is the frequency $\omega_s^2=\omega_0^2+\Omega_p^2/(\epsilon_A^{(\infty)}+\epsilon_B^{(\infty)})$, the frequency of the surface polariton which propagates on the single interface between a semi-infinite half-space filled with medium A, with the other side formed from medium B. From Eq. (2.23), one sees the $\omega_+(k,q)$ branch lies in the frequency regime $\omega_s\leq\omega_-\leq\omega_s$, while the ω_- branch lies in the regime $\omega_s\leq\omega_-\leq\omega_{\rm LO}$. If medium A is a metal, then $\omega_0\to0$, ω_s is the surface-plasma frequency, and $\omega_{\rm LO}$ becomes the bulk-plasma frequency of material A.

C. Semi-infinite superlattice; excitations localized near the surface

We now consider the geometry illustrated in Fig. 2. We have a superlattice structure identical to that in Fig. 1, but the structure is terminated at the plane $z=0$, with the half-space $z<0$ filled with material that has a dielectric constant $\epsilon_c(\omega)$.

As we remarked in Sec. I, terminating the superlattice structure destroys its periodicity in the z direction, so that we no longer have collective excitations with Bloch character in the z direction, as described by Eqs. (2.8) and

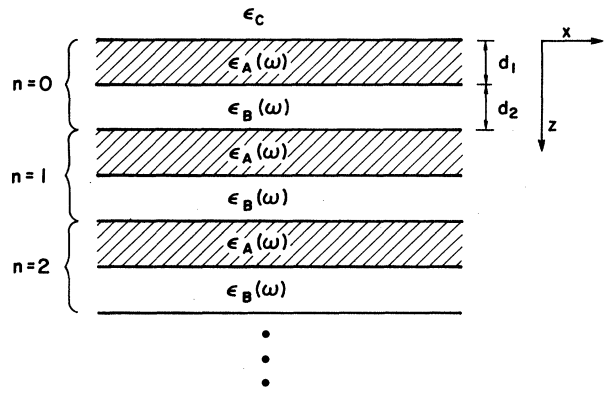

FIG. 2. Semi-infinite superlattice. The structure is made of alternating layers of material A and B as in Fig. 1, but the structure is terminated with the half-space $z<0$ filled with material C.

(2.9). There will surely be modes which may be viewed as propagating up to the surface from $z=+\infty$, then reflecting back into the superlattice structure, with a reflection coefficient that may be obtained by a suitable extension of the discussion in the preceding subsection. Here we will not be concerned with these modes, but instead with a new class of solutions that emerge. These modes have their excitation localized in the near vicinity of the interface between material C and the superlattice. One may view these new excitations as linear superpositions of surface modes localized to a particular interface, with an envelope function that decays exponentially as one moves into the stack.

The surface modes may be described by taking, for the electrostatic potential in the slab of material A in the region $nL<z<nL+d_1$, the form

$$\Phi(z)=e^{-\beta nL}(A_+e^{k(z-nL)}+A_-e^{-k(z-nL)}) , \tag{2.26}$$

while in medium B, in the region $nL+d_1<z<(n+1)L$, we shall have

$$\Phi(z)=e^{-\beta nL}(B_+e^{k(z-nL-d_1)}+B_-e^{-k(z-nL-d_1)}) . \tag{2.27}$$

Recalling that k is the magnitude of the wave vector parallel to the surface [Eq. (2.5)], the attenuation constant β will be determined in the subsequent analysis. Of course, we require $\mathrm{Re}(\beta)>0$.

In the region $z<0$, where material C resides, we have

$$\Phi(z)=Ce^{+kz} . \tag{2.28}$$

In our applications of the theory, we shall take $\epsilon_c(\omega)=1$ for simplicity, although the general formulas obtained below allow this parameter to take on any desired value.

We now turn to the boundary conditions. The four conditions at the interface $z=nL$ and $z=nL+d_1$ provide a set of relations for A_+, A_-, B_+, and B_- identical to those in Eqs. (2.13)–(2.16), except iq is replaced everywhere by $-\beta$. It is convenient to eliminate B_+ and B_- from these equations in order to reduce the set to two equations which involve only A_+ and A_-. We have, once this is done,

$$\left[1+\frac{\epsilon_A}{\epsilon_B}\right](e^{kd_1}-e^{-\beta L}e^{-kd_2})A_+ + \left[1-\frac{\epsilon_A}{\epsilon_B}\right](e^{-kd_1}-e^{-\beta L}e^{-kd_2})A_-=0 \tag{2.29}$$

and

$$\left[1-\frac{\epsilon_A}{\epsilon_B}\right](e^{kd_1}-e^{-\beta L}e^{kd_2})A_+ + \left[1+\frac{\epsilon_A}{\epsilon_B}\right](e^{-kd_1}-e^{-\beta L}e^{kd_2})A_-=0 . \tag{2.30}$$

We have dropped explicit reference to the frequency dependence of the dielectric constants for convience. For Eqs. (2.29) and (2.30) to be satisfied with A_+ and A_- nonzero, the appropriate 2×2 determinant must vanish, leading to a constraint on the attenuation constant β. One must have

$$\cosh(\beta L)=\cosh(kd_1)\cosh(kd_2) + \frac{1}{2}\left[\frac{\epsilon_A}{\epsilon_B}+\frac{\epsilon_B}{\epsilon_A}\right]\sinh(kd_1)\sinh(kd_2) , \tag{2.31}$$

a relation equivalent to Eq. (2.17) with q replaced by $i\beta$.

Further constraints are obtained by requiring the boundary conditions to be satisfied at the interface $z=0$. These give simply

$$C=A_++A_- \tag{2.32}$$

and

$$\epsilon_cC=\epsilon_A(A_+-A_-) , \tag{2.33}$$

or with C eliminated, we have a new equation which involves A_+ and A_-,

$$\left[1-\frac{\epsilon_A}{\epsilon_c}\right]A_+ + \left[1+\frac{\epsilon_A}{\epsilon_c}\right]A_-=0 . \tag{2.34}$$

We have three unknowns, A_+, A_-, and β, and Eqs. (2.29), (2.30), and (2.34) provide three constraint equations. Upon combining Eqs. (2.30) and (2.34), we have

$$e^{-\beta L}=e^{-kd_2}[\cosh(kd_1)+P_1\sinh kd_1] , \tag{2.35}$$

where

$$P_1=\frac{\epsilon_A^2-\epsilon_B\epsilon_c}{\epsilon_A(\epsilon_c-\epsilon_B)} ,$$

while we may also combine Eq. (2.29) with Eq. (2.34) to find a second relation for $\exp(-\beta L)$,

$$e^{-\beta L}=e^{+kd_2}[\cosh(kd_1)+P_2\sinh(kd_1)] , \tag{2.36}$$

where

$$P_2=\frac{\epsilon_A^2+\epsilon_B\epsilon_c}{\epsilon_A(\epsilon_c+\epsilon_B)} . \tag{2.37}$$

The right-hand side of Eq. (2.35) must equal the right-hand side of Eq. (2.36), so that we have the final constraint

$$2\cosh(kd_1)\sinh(kd_2) + \sinh(kd_1)[P_2 e^{kd_2} - P_1 e^{-kd_2}] = 0 . \quad (2.38)$$

Equation (2.38) constitutes an implicit dispersion relation for the surface wave. Once this is solved, we must then check the value of β as found, say, from Eq. (2.35), to be certain that $\mathrm{Re}(\beta) > 0$.

At this point, we may turn to a number of special cases. Let us suppose for definiteness that both ϵ_B and ϵ_c may be regarded as frequency independent in the spectral regime of interest, while it is $\epsilon_A(\omega)$ that varies with frequency. Then after some manipulation, Eq. (2.38) may be used to generate a quadratic equation satisfied by $\epsilon_A(\omega)$,

$$\sinh(kd_1)[\epsilon_B\cosh(kd_2) - \epsilon_c\sinh(kd_2)]\epsilon_A^2(\omega) + (\epsilon_B^2 - \epsilon_c^2)\cosh(kd_1)\sinh(kd_2)\epsilon_A(\omega) + \epsilon_B\epsilon_c\sinh(kd_1)[\epsilon_B\sinh(kd_2) - \epsilon_c\cosh(kd_2)] = 0 , \quad (2.39)$$

so that the possible frequencies of the surface modes are such that

$$\epsilon_A(\omega) = \frac{-1}{2\sinh(kd_1)[\epsilon_B\cosh(kd_2) - \epsilon_c\sinh(kd_2)]} \times ((\epsilon_B^2 - \epsilon_c^2)\cosh(kd_1)\sinh(kd_2) \pm \{(\epsilon_B^2 - \epsilon_c^2)^2\cosh^2(kd_1)\sinh^2(kd_2) + 2\epsilon_B\epsilon_c\sinh^2(kd_1)[2\epsilon_B\epsilon_c\cosh(2kd_2) - (\epsilon_B^2 + \epsilon_c^2)\sinh(2kd_2)]\}^{1/2}) . \quad (2.40)$$

A particularly striking special case is that for which $\epsilon_B \equiv \epsilon_c$. For a semi-inifinite stack of films formed from a "surface active medium" (i.e., one with a negative dielectric constant in certain spectral regions) separated by vacuum, with vacuum above, we have $\epsilon_B = \epsilon_c = 1$. Then Eq. (2.40) reduces to the simple pair of statements

$$\epsilon_A(\omega) = \pm\epsilon_B . \quad (2.41a)$$

If we choose the upper sign, we see that $\beta = -k$, an unacceptable value. However, if

$$\epsilon_A(\omega) = -\epsilon_B , \quad (2.41b)$$

we have

$$\beta = k\frac{d_1 - d_2}{L} , \quad (2.41c)$$

which is quite acceptable if $d_1 > d_2$.

The condition in Eq. (2.41b) is *precisely the same* as that which determines the surface-polariton frequency, in the neglect of retardation, on the interface between a semi-infinite slab of material B joined with a *semi-infinite* slab of material A. The penetration constant β differs, however, in that one has $\beta = k$ when $d_2 = 0$, and only material A resides in the upper half-space $z > 0$. For our problem, we see that β decreases to zero as $d_2 \to d_1$ from below, and no surface wave exists when $d_2 > d_1$. This mode is a precise analog to the surface spin wave of the magnetic superlattice discussed in earlier papers,[3,4] and which has also been studied experimentally.[4,5] We shall explore this wave further in the next subsection, where its relation to the bulk excitation spectrum of the superlattice structure will be elucidated.

D. Some explicit examples of superlattice excitation spectra

Here we present some numerical studies of the dispersion relations of collective excitations in semi-infinite superlattice structures. In what follows, we suppose $\epsilon_A(\omega) = 1 - \omega_p^2/\omega^2$, with $\omega_p = 15$ eV. This corresponds to a model of aluminum. For ϵ_c, we choose unity, so that we have a semi-infinite stack of aluminum films separated by a dielectric space with a dielectric constant ϵ_B.

In Fig. 3 we show dispersion curves where $d_1 = 2d_2$, and $\epsilon_B = 1$. We see that the bulk excitations described in Sec. II B fall into two bands separated by a gap. Note that as one scans through the frequency spectrum of bulk modes with a finite wave vector $\vec{k}$ parallel to the surface, the modes tend to crowd together, forming a high density of states near the boundary lines with $qL = \pi$.

In Figs. 4(a) and 4(b), for two values of the parameter kd_1, we illustrate frequencies of the collective modes of the semi-infinite superlattices as a function of the ratio d_1/d_2. The ω_+ and ω_- bulk bands [Eq. (2.23)] are always separated by a gap, except for the special case $d_1 = d_2$, where their lower bounds just touch. The surface mode always lies within this gap, but it exists only when $d_1 > d_2$, as one sees from our earlier discussion.

A diverse variety of collective-mode spectra may be found, depending on the nature of the two constituents. Figure 5 illustrates the effect of an insulating spacer placed between the Al model films. We still have $\epsilon_c = 1$ in this figure, but now $\epsilon_B = 3$, a reasonable value for Al_2O_3 or some other wide-gap insulator. For large values of kd_1, both the ω_+ and ω_- bulk modes are down-shifted in frequency by virtue of the screening provided by the oxide. For large values of kd_1, the surface branch lies near the surface-mode frequency appropriate to the Al/vacuum interface, 10.6 eV. Thus, in contrast to the earlier example, the surface mode lies *above* the ω_+ bulk-wave branch. As

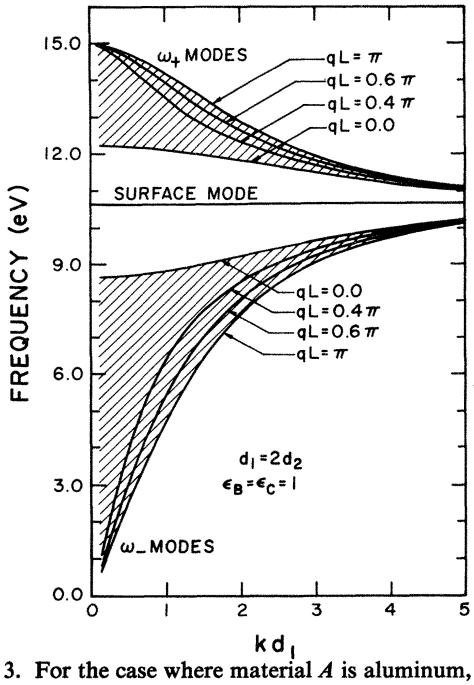

FIG. 3. For the case where material A is aluminum, and both dispersion relation of the surface mode of the semi-infinite superlattice, and those of the bulk modes described in Sec. II B of the text.

kd_1 decreases, this mode merges with the ω_+-mode continuum at $kd_1 \cong 1.5$, for this choice of d_2. On this branch, we have $\beta L = i\pi + \chi$, were χ assumes the value 6.37 at $kd_1 = 5.0$, then decreases monotonically to reach zero as the surface mode merges with the bulk continuum. Then, at smaller values of kd_1, we find a surface mode that lies in the gap between the ω_- and ω_+ bulk branches. This mode also merges with the ω_+ continuum at a wave vector very close to that where the high-frequency branch does. On the low-frequency surface-mode branch, βL is purely real, and vanishes as the critical wave vector is approached from below.

In contrast to the simple case where $\epsilon_B = \epsilon_c$, when $\epsilon_B > \epsilon_c$ we find surface waves of the structure when $d_1 < d_2$. This is illustrated in Fig. 6, where, for the choice $d_2 = \frac{1}{2}d_1$, we give the excitation spectrum of the superlattice structure with $\epsilon_c = 1$ and $\epsilon_B = 3$. We have a high-frequency branch of surface waves, again with $\beta = i\pi + \chi$. This branch behaves in a manner qualitatively similar to the upper branch in Fig. 5. We also have a second surface wave in the gap between the ω_+ and ω_- bulk branches again (with β real as before), but now the branch does not merge with the bulk excitations as kd_1 increases to a critical value. As far as we can tell, the surface mode survives in the limit $kd_1 \to \infty$, always "trapped" between the two bulk branches. Quite clearly, we have a rich spectrum of elementary excitations in these structures, depending on the nature of the constituents and their relative thickness.

III. INELASTIC ELECTRON SCATTERING FROM COLLECTIVE EXCITATIONS OF SUPERLATTICES

In Sec. II we presented the theory of the collective excitations of superlattice structures. We next turn to the question of how their properties may be studied. If we are concerned with metallic superlattices, possibly with insulating spacers between adjacent metal films, then small-

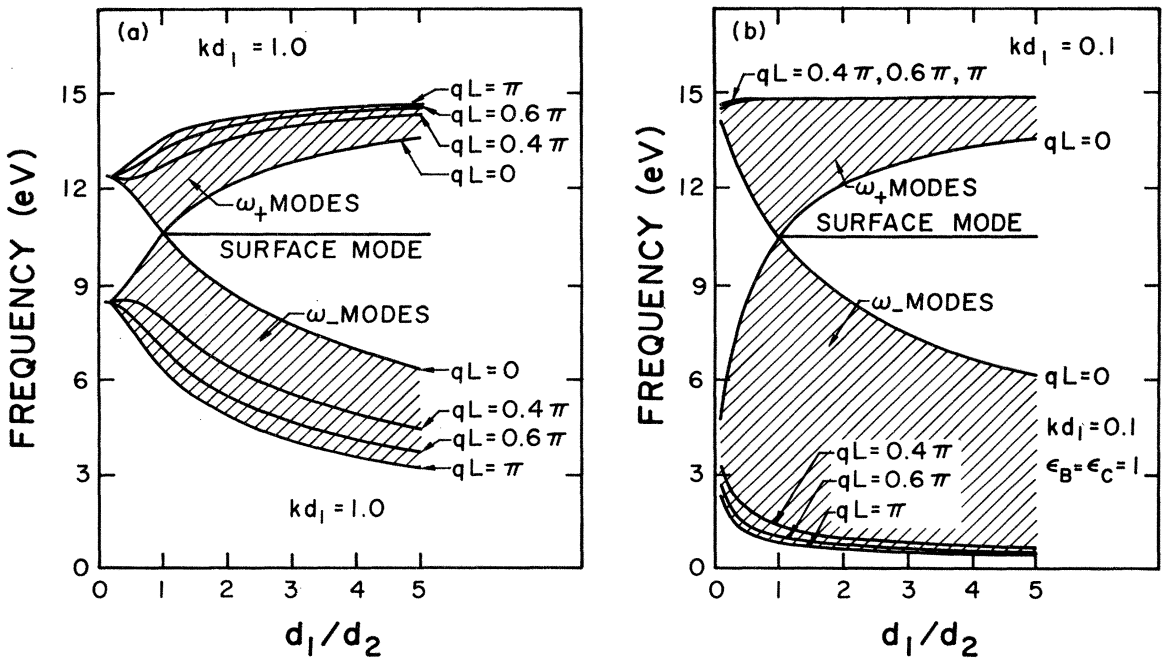

FIG. 4. For the case $\epsilon_B = \epsilon_c = 1$, we show, for (a) $kd = 1.0$ and (b) $kd = 0.1$, the frequency spectrum of the bulk ω_+ and ω_- bands of the semi-infinite superlattice along with the surface mode. The surface mode is absent when $d_2 > d_1$, as discussed in the text.

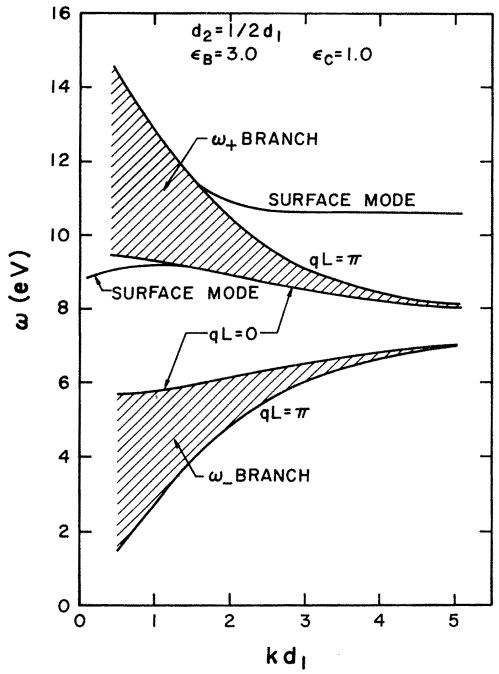

FIG. 5. For the case $\epsilon_B = 3$ and $\epsilon_c = 1$, we give the collective-mode frequencies as a function of wave vector for the case $d_1 = 2d_2$. Material A is aluminum, modeled as described in the text.

angle inelastic electron scattering may serve as a suitable experimental probe since it has been used to study surface excitations on metal surfaces.[8] Since the losses of interest lie in the range of several electron volts, very-high-resolution techniques are not required. In this section we present the theory of electron-energy loss in a reflection geometry for small-angle inelastic scattering from a semi-infinite superlattice.

In the regime of small-angle deflections, where surface-plasmon contributions dominate the loss spectrum for

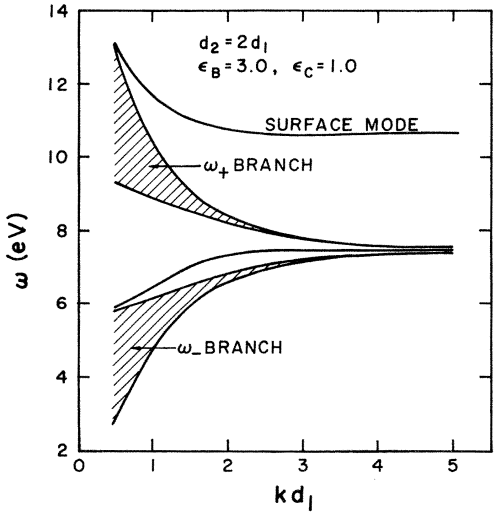

FIG. 6. For $\epsilon_B = 3$ and $\epsilon_c = 1$, we give the superlattice collective-mode spectrum as a function of wave vector for $d_1 = \frac{1}{2} d_2$. Again, material A is aluminum.

back scattering off of the surface of a simple metal, the electron interacts with the excitations in the substrate through the fluctuating electric fields in the vacuum outside the substrate. The theory of the loss cross section under this circumstances was discussed some years ago for scattering off the surface of a semi-infinite material,[9] or for a material upon which an optically active overlayer is present.[10] A summary of this theory, along with a number of applications of the resulting formulas, may be found in a recent book.[11]

Here we wish to extend the theory to the superlattice structures discussed in Sec. II. We could do so by following the quantum-mechanical analyses given earlier, but Schaich[12] has used a simple classical trajectory procedure which reproduces one limiting form of the results provided by the full analysis. One must note that this limiting form follows from a full treatment only after certain assumptions are introduced;[9,11] these are of questionable validity when the energy loss of the electron is in the range of several electron volts, but the classical trajectory analysis yields a formula which surely contains the principal features expected in the data.

The trajectory analysis proceeds by noting that the incoming electron polarizes the substrate, here viewed as a dielectric medium. The induced polarization produces an electric field which does work on the electron as it approaches the crystal, and then exits after reflection off the surface. One calculates the total work performed by the induced field to obtain the total energy loss suffered by the electron, and an appropriate decomposition of this expression yields the energy distribution of those electrons which suffer an inelastic scattering.

Let the electron trajectory be described by $\vec{x}(t) = \vec{x}_{||}(t) + \hat{z} z(t)$, with $\vec{x}_{||}$ the projection of $\vec{x}$ onto a plane parallel to the surface. We may calculate the electric field generated by the induced polarization by solving Laplace's equation in the vacuum above the sample,

$$\nabla^2 \phi(\vec{x},t) = -4\pi e\, \delta(\vec{x}_{||} - \vec{x}_{||}(t)) \delta(z - z(t)) , \tag{3.1}$$

with the electrostatic potential subject to appropriate boundary conditions at the surface. We ignore the fact that the electron penetrates into the substrate. In the substrate, since there is no free charge, we have

$$\nabla^2 \phi(\vec{x},t) = 0 . \tag{3.2}$$

Also, $\vec{x}_{||}(t) = \vec{v}_{||} t$ for $-\infty < t < +\infty$, with $\vec{v}_{||}$ the projection of the electron's velocity on a plane parallel to the surface.

We may write

$$\phi(\vec{x}_{||},z;t) = \int \frac{d^2 Q_{||}}{(2\pi)^2} \phi(\vec{Q}_{||},z;t) e^{i \vec{Q}_{||} \cdot \vec{x}_{||}} , \tag{3.3}$$

and one easily that $\phi(\vec{Q}_{||},z;t)$ satisfies

$$\left[\frac{d^2}{dz^2} - Q_{||}^2 \right] \phi(\vec{Q}_{||},z;t) = -4\pi e\, \delta(z - z(t)) e^{-i \vec{Q}_{||} \cdot \vec{v}_{||} t} \tag{3.4}$$

in the vacuum outside the material and the homogeneous version of Eq. (3.4) within the material. If the electron strikes the surface at $t=0$, then

$$z(t)=\begin{cases} v_\perp t & \text{for } t<0\ , \\ -v_\perp t & \text{for } t>0\ . \end{cases} \tag{3.5}$$

As in Sec. II, the sample occupies the half-space $z<0$. If we write

$$\phi(\vec{Q}_{||},z;t)=\int_{-\infty}^{+\infty}\frac{d\omega}{2\pi}\phi(\vec{Q}_{||},z;\omega)e^{-i\omega t}\ , \tag{3.6}$$

one finds that $\phi(\vec{Q}_{||},z;\omega)$ obeys

$$\left[\frac{d^2}{dz^2}-Q_{||}^2\right]\phi(\vec{Q}_{||},z;\omega)=-\frac{8\pi e}{v_\perp}\cos\left[(\omega-\vec{v}_{||}\cdot\vec{Q}_{||})\frac{z}{v_\perp}\right]\ , \tag{3.7}$$

and the homogeneous form in the medium.

A particular solution of Eq. (3.7) in the half-space $z>0$ is

$$\phi_p(\vec{Q}_{||},z;\omega)=A(\vec{Q}_{||},\omega)\cos\left[(\omega-\vec{v}_{||}\cdot\vec{Q}_{||})\frac{z}{v_\perp}\right]\ , \tag{3.8}$$

where

$$A(\vec{Q}_{||},\omega)=\frac{8\pi e}{(\omega-\vec{Q}_{||}\cdot\vec{v}_{||})^2+Q_{||}^2v_\perp^2}\ . \tag{3.9}$$

We have to append to Eq. (3.8) a general solution to the homogeneous form of Eq. (3.7), and then match the resulting form to the solution of Laplace's equations in the sample, so that the proper boundary conditions are obeyed at each interface. We shall suppress reference to the dependence of various quantities on $\vec{Q}_{||}$ and ω for brevity. Thus, in the region $z<0$ below the sample, here assumed to be vacuum ($\epsilon_c=1$ in the notation of Sec. II), we have

$$\phi(z)=A\cos\left[(\omega-\vec{Q}_{||}\cdot\vec{v}_{||})\frac{z}{v_\perp}\right]+C_+e^{Q_{||}z}\ , \tag{3.10}$$

while, as in Sec. II, the most general form of the potential in the outermost superlattice layer is

$$\phi(z)=A_+e^{Q_{||}z}+A_-e^{-Q_{||}z},\quad 0\le z\le d\ . \tag{3.11}$$

The term proportional to C_+ in Eq. (3.10) generates the induced field which does work on the electron.

Continuity of the total potential and normal component of $\vec{D}$ at $z=0$ gives the two conditions

$$A_++A_-=A+C_+ \tag{3.12a}$$

and

$$\epsilon_A(\omega)(A_+-A_-)=C_+\ . \tag{3.12b}$$

If the second constituent of the superlattice is described by the dielectric constant ϵ_B, as in Sec. II, then from the discussion given there we know that

$$A_+=FA_-\ , \tag{3.13a}$$

where

$$F=+\left[\frac{\epsilon_A+\epsilon_B}{\epsilon_A-\epsilon_B}\right]\left[\frac{e^{-Q_{||}d_1}-e^{-\beta L}e^{Q_{||}d_2}}{e^{Q_{||}d_1}-e^{-\beta L}e^{Q_{||}d_2}}\right]\ , \tag{3.13b}$$

with β determined from Eq. (2.30), after k is replaced by $Q_{||}$. The condition $\mathrm{Re}\beta>0$ is appended.

From Eqs. (3.12), we then find an expression for C_+,

$$C_+=\frac{-\epsilon_AA(F-1)}{(\epsilon_A-1)F-(\epsilon_A+1)}\equiv RA\ . \tag{3.14}$$

It is a straightforward matter to use the electric field generated from the term $C_+\exp(Q_{||}z)$ in Eq. (3.10) to calculate the work done on the electron by the induced field. The work performed by this source has a magnitude

$$W=\frac{2e^2v_\perp^2}{\pi^2}\int_{-\infty}^{\infty}\frac{d^2Q_{||}d\omega Q_{||}\omega}{[(v_\perp Q_{||})^2+(\omega-\vec{v}_{||}\cdot\vec{Q}_{||})^2]}\mathrm{Im}[R(Q_{||},\omega)]\ , \tag{3.15}$$

where

$$R(Q_{||},\omega)=\frac{\epsilon_A(\omega)(F-1)}{[\epsilon_A(\omega)-1]F-[\epsilon_A(\omega)+1]}\equiv 1-\frac{1}{1+\epsilon_A(\omega)(1-F)/(1+F)}\ . \tag{3.16}$$

The expression for the energy lost by the electron may be cast into the form

$$W=\int_0^\infty d\omega\,\hbar\omega P(\omega)\ , \tag{3.17}$$

where $P(\omega)$ is interpreted as the probability per unit frequency that the electron has lost the energy $\hbar\omega$. We then have, noting that $\mathrm{Im}[R(\vec{Q}_{||},\omega)]$ is an odd function of frequency,

$$P(\omega)=\frac{e^2v_\perp^2}{\hbar\pi^2}\int\frac{d^2Q_{||}Q_{||}\mathrm{Im}[R(Q_{||},\omega)]}{[(v_\perp Q_{||})^2+(\omega-\vec{v}_{||}\cdot\vec{Q}_{||})^2]^2}\ . \tag{3.18}$$

Upon noting that $R(Q_{||},\omega)$ depends only on the magnitude and note the direction of $\vec{Q}_{||}$, we may write

$$P(\omega)=\frac{e^2v_\perp^2}{\hbar\pi^2}\int dQ_{||}Q_{||}^2\mathrm{Im}[R(Q_{||},\omega)]\times\int_0^{2\pi}d\theta\frac{1}{[(v_\perp Q_{||})^2+(\omega-Q_{||}v_{||}\cos\theta)^2]^2}\ . \tag{3.19}$$

The integral on θ may be evaluated in closed form. Since this integral is encountered frequently in the theory of small-angle electron-energy loss, we shall quote the result explicitly. Let θ_I be the angle of incidence of the

electron beam measured relative to the normal to the surface. Then

$$v_{||}=v_0\sin\theta_I \tag{3.20a}$$

and

$$v_{\perp}=v_0\cos\theta_I\ , \tag{3.20b}$$

where v_0 is the speed of the incoming electron. The result is conveniently expressed in terms of the dimensionless variable ξ given by

$$\xi=v_0Q_{||}/\omega\ . \tag{3.21}$$

The loss function then becomes,

$$P(\omega)=\frac{v_0^2e^2}{\pi\hbar\omega^4\cos^2\theta_I}\int\frac{dQ_{||}Q_{||}^2\mathrm{Im}[R(Q_{||},\omega)]}{\xi^3[(\xi^2-1)^2+4\xi^2\cos^2\theta_I]^{3/2}}$$

$$\times\mathrm{Re}\{(\xi^2-1+2i\xi\cos\theta_I)^{1/2}[(1+2\xi^2\cos\theta_I+i\xi\cos\theta_I)(1+\xi^2\cos^2\theta_I)$$

$$+\xi^2\sin^2\theta_I(3\xi^2\cos^2\theta_I-2-i\xi\cos\theta_I)+\xi^4\sin^4\theta_I]\}\ . \tag{3.22}$$

In the calculation of the loss cross section, the integral on the magnitude of $Q_{||}$ quite clearly must be performed numerically. But our analytic evaluation of the angular integration in Eq. (3.19) reduces this to a simple task, outlined below, since the calculation involves integration over only one variable.

It should be noted that for $R(Q_{||},\omega)$ to be nonzero, one or more of the dielectric constants of the substrate must have a nonzero imaginary part. In our study of the dispersion relations in Sec. II, all dielectric constants were taken to be real. Thus, here the attenuation constant β, as found from Eq. (2.31), has a nonzero real and imaginary part, and care must be taken to always choose β so that $\mathrm{Re}\beta>0$. In the calculations reported in Sec. IV, the aluminum film is modeled by the choice

$$\epsilon_A(\omega)=1-\frac{\omega_p^2}{\omega(\omega+i\gamma)}\ , \tag{3.23}$$

with γ the conduction-electron relaxation rate.

Near-specular electron-energy-loss studies generally collect not all the electrons scattered via the mechanism described above, but rather collect those scattered within a certain angular range about the specular direction. This range is determined by the slit width of the spectrometer, which generally subtends an angle of roughly 1°, as viewed from the sample. In our calculations, we simulate this by cutting off the integral on $Q_{||}$ in Eq. (3.22) at the value $Q_{||}^{(c)}=k^{(I)}\Delta\theta$, with $k^{(I)}$ the wave vector of the incident electron. In the scattering event, $\hbar Q_{||}$ is the momentum transfer suffered by the electron projected onto a plane parallel to the surface, so that this procedure assumes that all electrons which suffer a momentum transfer (projected onto a plane parallel to the surface) between 0 and $Q_{||}^{(c)}$ are collected. One could envision a more realistic cutoff procedure, reflecting the actual slit geometry, but this method allows the integration on θ to be performed analytically, as described above. The results of the calculation are not very sensitive to the details of the cutoff procedure.

IV. NUMERICAL CALCULATION OF THE ELECTRON-ENERGY-LOSS CROSS SECTION—GENERAL DISCUSSION

We now turn to our numerical studies of the electron-energy-loss cross section for scattering off a superlattice structure.

We first consider the case where $\epsilon_B=1$, since, as we see from Sec. II, the excitation spectrum for this case is particularly simple. In the figures that follow, we choose the incident-electron kinetic energy to be 200 eV, with a 45° angle of incidence. The spectrometer slit widths are assumed equal to 1°, as mentioned at the end of Sec. IV. Material A is modeled through use of the dielectric function in Eq. (3.23), with $\omega_p=15$ eV and $\gamma=0.2$ eV

In Fig. 7, we show the loss spectrum for two cases: The first has $d_1=20$ Å and $d_2=15$ Å, while the second has $d_1=15$ Å and $d_2=20$ Å. Clearly visible is the prominent surface-mode peak at 10.6 eV for the former case, while only a hole is present for the latter, near the aluminum/vacuum surface-plasmon frequency of 10.6 eV. The broad feature which rises dramatically with decreasing energy loss has its origin in scattering off of the continuum of "bulk" excitations which, as one sees from Fig. 3, extend down to very low frequency when $Q_{||}d_1$ is small. This feature will be evident in data as a broadening of the quasielastic peak, which varies as the thickness of the aluminum film is changed. Such a broadening of the quasielastic peak is evident in recent studies of thin films of Ag deposited on GaAs;[13] here the whole feature is shifted to much lower energies by virtue of the smaller bulk-plasmon frequency of Ag and by softening of the low-frequency collective modes of Ag produced by the screening of the electric fields provided by the GaAs substrate. A theory identical to that employed here provides an excellent account of the variation of the broadening with increasing Ag film thickness. Note, that as in the earlier example,[13] with increasing aluminum film thickness, the intensity of the quasielastic background decreases for films thicker than a few monolayers.

It is well known that if one scatters electrons off a semi-infinite sample of aluminum, then the mechanism

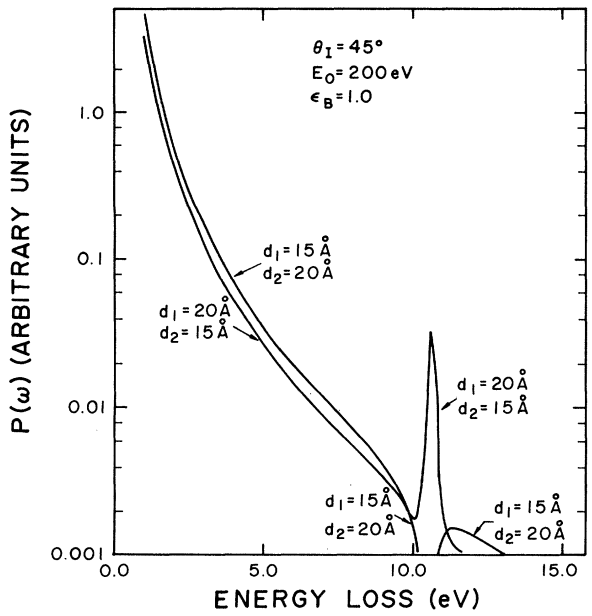

FIG. 7. Electron-energy-loss cross section for near-specular scattering of 200-eV electrons off of a semi-infinite superlattice of very thin aluminum films interspersed with vacuum. Two cases, as indicated, are considered.

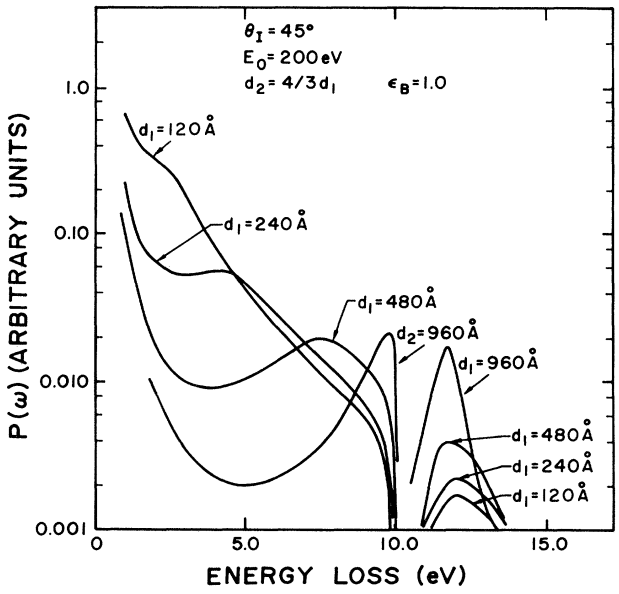

FIG. 8. Electron-energy-loss cross section for near-specular scattering of 200-eV electrons from a semi-infinite superlattice of aluminum films with vacuum in between. In all cases, the ratio d_2/d_1 is fixed at the value $\frac{4}{3}$.

considered here leads to a loss peak at the frequency of the surface mode of the aluminum/vacuum interface, 10.6 eV for our model. It is interesting to inquire how such a spectrum evolves from that given in Fig. 7 if d_1 is increased with the ratio d_2/d_1 held fixed at a value greater than unity; the point is that in the limit $d_1 \to \infty$, we must have a loss peak at 10.6 eV as the only feature in the spectrum, but the discussion of Sec. II shows we never have a surface mode at this frequency for any finite value of d_1 if d_2/d_1 is greater than unity (see Fig. 4).

We study this point in Fig. 8, where we show the energy-loss cross section for several values of d_1 with the ratio d_1/d_2 fixed and d_1 increasing to rather large values. For $d_1 = 120$ Å, we see a shoulder near 2.5 eV produced by scattering off the ω_- branch of excitations. As d_1 increases, this shoulder evolves into a prominent peak, and moves to progressively higher energy, but always below 10.6 eV. Similarly, scattering from the ω_+ branch produces a loss peak above 10.6 eV which softens as d_1 increases, always remaining above 10.6 eV. As d_1 increases, the two peaks coalesce, and the gap between them fills in. What is left in the limit $d_1 \to \infty$ with d_2/d_1 fixed at a value greater than unity is a single feature centered at 10.6 eV with a width controlled by the damping factor γ in Eq. (3.23). Note that as d_1 increases, the low-energy "tail" in the loss spectrum decreases dramatically, so that there will be very little broadening of the quasielastic beam for scattering off thick films.

Upon comparing the dramatic differences between the energy-loss spectra in Figs. 7 and 8, one may appreciate that even when the aluminum film is quite thick, the electron-energy-loss spectrum is influenced by the whole structure and not just by the properties of its outermost constituent. This point is reinforced in Fig. 9, where we present calculations, again with $\epsilon_B = 1$, of the loss spectrum for several values of d_1, but now with the ratio d_2/d_1 fixed at $\frac{3}{4}$ rather than $\frac{4}{3}$.

In Fig. 10 we present calculations of the loss spectrum for scattering from a semi-infinite stack of aluminum films, but now with each separated by a dielectric with a dielectric constant $\epsilon_B = 3$. In each example, the low-frequency loss peak has its origin in scattering off the surface excitation in the gap between the ω_+ and ω_- bulk ex-

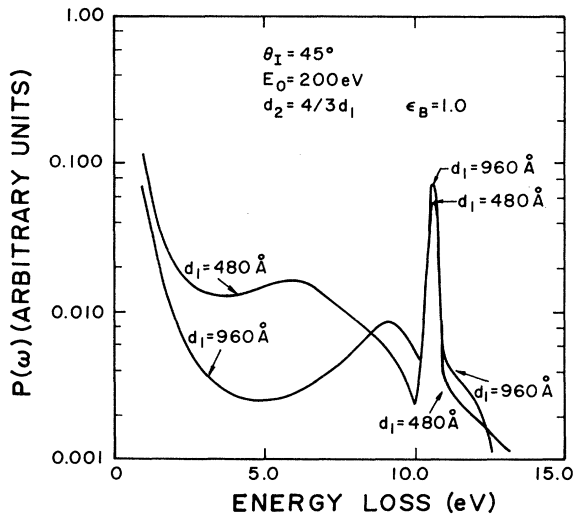

FIG. 9. Electron-energy-loss cross section for near-specular scattering of 200-eV electrons from a semi-infinite superlattice of aluminum films with vacuum in between. In all cases, the ratio d_2/d_1 is fixed at the value $\frac{3}{4}$.

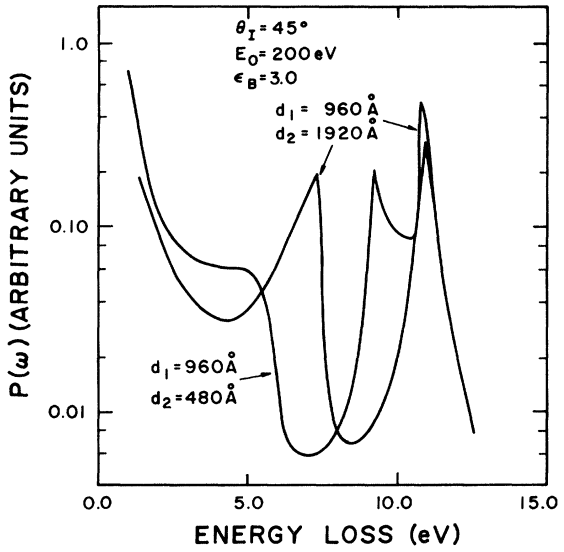

FIG. 10. For $\epsilon_B = 3$, and two sets of values for d_1 and d_2, we show the energy-loss spectrum, with material A again chosen to be aluminum.

citation branches. For the case $d_2 = \frac{1}{2}d_1$, the surface wave which exists only for a limited range of wave vectors evidently scatters electrons with sufficient intensity to produce a clear loss peak. The high-frequency feature in the loss spectrum has its origin in scattering off of the upper surface wave branch; the peak in each case is shifted somewhat above the 10.6-eV loss energy appropriate to the Al/vacuum interface. The origin of this shift is the upward dispersion evident in Figs. 5 and 6. Again, one appreciates from the figure that the loss spectrum reflects the nature of the structure below the outermost aluminum film, even for rather thick films.

While we have confined our attention to the case of a superlattice with a metallic and an insulating material as the two constituents of the semi-infinite superlattice in our numerical examples, the theory quite clearly applies to semiconducting superlattice structures as well. For this reason, in Secs. II and III we have attempted to present the analysis in a sufficiently generalized form so that the interested reader may apply the theory to any structure of interest. We note, in fact, that electron-energy-loss spectroscopy has been applied to the study of the surface excitations of doped GaAs,[14] so that it should also prove a suitable probe of superlattices, although high-resolution methods are now required since the losses of interest lie in the range of a few tens of meV. Perhaps Raman spectroscopy will also prove a powerful probe of the modes discussed here in semiconducting systems. We currently have semiconducting superlattices under study and the results will be reported elsewhere.

ACKNOWLEDGMENTS

This research has been supported by the U. S. National Aeronautics and Space Administration through Contract No. NAG3-250.

[1]See, for example, Z. Q. Zheng, C. M. Falco, J. B. Ketterson, and I. K. Schuller, Appl. Phys. Lett. 38, 424 (1981).
[2]A. L. Fetter, Ann. Phys. (N.Y.) 88, 1 (1974).
[3]R. E. Camley, T. S. Rahman, and D. L. Mills, Phys. Rev. B 27, 261 (1983).
[4]P. Grünberg and R. Mika, Phys. Rev. B 27, 2955 (1983).
[5]M. Grimsditch, M. Khan, A. Kueny, and I. K. Schuller, Phys. Rev. Lett. 51, 498 (1983).
[6]We understand the influence of retardation on the excitations of superlattice structures is under investigation by G. Giuliani, J. J. Quinn, and R. F. Wallis (unpublished).
[7]E. Evans and D. L. Mills, Phys. Rev. B 8, 4004 (1973).
[8]C. Powell, Phys. Rev. 175, 972 (1968).
[9]D. L. Mills, Surf. Sci. 48, 59 (1975).
[10]H. Froitzheim, H. Ibach, and D. L. Mills, Phys. Rev. B 11, 1980 (1975).
[11]H. Ibach and D. L. Mills, *Electron Energy Loss Spectroscopy and Surface Vibrations* (Academic, San Francisco, 1982), Chap. 3.
[12]W. L. Schaich, Phys. Rev. B 24, 686 (1981).
[13]L. H. Dubois, G. P. Schwartz, R. E. Camley, and D. L. Mills (unpublished).
[14]R. Matz and H. Luth, Phys. Rev. Lett. 46, 500 (1981).